

# Chapter Five

## *Wavelength-Dispersive X-ray Spectrometers*

### 5. Introduction

In this chapter we present the details of Wavelength-Dispersive X-ray Spectrometers (WDS) that form the foundation for quantitative chemical analysis with EPMA instruments. We will first review some of the factors that govern the generation of x-rays and the intensities of x-rays that are produced during electron-beam bombardment. We will then examine the spectrometers and electronics necessary to acquire x-ray intensities.

### 5.1 Selection of Beam Energy

For x-ray analysis the minimum useful beam energy is determined by the critical energy ( $E_C$ ) required to excite the inner shell ionizations that give rise to the characteristic lines of interest. Examples for typical elements are listed in Table 5-1 below (all energies are given in keV).

In Table 5-1 we see (in bold type) that  $E_0 = 15\text{keV}$  suffices to excite the K lines for elements up to, but not including, Rb ( $Z=37$ ) and the  $L_\beta$  lines for elements up to, but not including, Fr ( $Z=87$ ). For the K and L lines of heavier elements, an accelerating potential greater than 15 keV is necessary.

The intensity of the characteristic x-ray lines of an element emerging from the specimen depends on many factors. The most important factor from our point of view is the concentration (number of atoms actually) of an element in the specimen, since that is the basis for quantitative x-ray analysis. Other factors affecting x-ray intensity include 1) the fluorescent yield (?) of the element, 2) beam current ( $i_b$ ), 3) loss of ionization due to backscattering and absorption of x-rays in the specimen, 4) secondary excitation (x-ray fluorescence) in the specimen, and 5) the difference between  $E_0$  and  $E_C$ .

The latter factor ( $E_0 - E_C$ ) is determined by selecting  $E_0$  of the electron gun. We typically perform most of our analyses at 10-20 keV, depending on the specimen and the elements and x-ray lines of interest. Special circumstances, for example, very thin films or trace element analysis might take us below or above that normal range of operation.

<b>Z</b>	<b>E<sub>C,K</sub></b>	<b>E<sub>K?1</sub></b>	<b>E<sub>L3</sub></b>	<b>E<sub>LA1</sub></b>
11 (Na)	<b>1.072</b>	<b>1.041</b>	-	-
14 (Si)	<b>1.840</b>	<b>1.740</b>	-	-
20 (Ca)	<b>4.038</b>	<b>3.692</b>	<b>0.342</b>	<b>0.341</b>
26 (Fe)	<b>7.111</b>	<b>6.404</b>	<b>0.707</b>	<b>0.705</b>
32 (Ge)	<b>11.10</b>	<b>9.886</b>	<b>1.217</b>	<b>1.188</b>
37 (Rb)	15.20	13.42	<b>1.806</b>	<b>1.694</b>
40 (Zr)	18.00	15.78	<b>2.223</b>	<b>2.042</b>
47 (Ag)	25.53	22.16	<b>3.351</b>	<b>2.984</b>
57 (La)	38.89	33.44	<b>5.484</b>	<b>4.651</b>
71 (Lu)	63.31	54.07	<b>9.249</b>	<b>7.656</b>
79 (Au)	80.73	68.80	<b>11.93</b>	<b>9.713</b>
87 (Fr)	101.1	86.10	15.02	12.03
92 (U)	115.6	98.47	17.16	13.62

Table 5-1. Energy range for x-rays excited by 15keV.

The dependence of the intensity of a characteristic x-ray line (peak) with  $(E_o - E_c)$  has an exponential form and is generally expressed as:

$$I_p \propto (E_o - E_c)^{1.7}$$

eq. 5-1

Recall that in addition to generating characteristic x-ray photons, electron-beam bombardment also produces a "continuum" or background radiation. The intensity of the continuum is also dependent on  $E_o$ . At the energy of any characteristic x-ray peak ( $E_p$ ), the background intensity can be written as follows:

$$I_b \propto (E_o - E_p)$$

eq. 5-2

The "**peak to background**" intensity ratio is a measure of the usefulness of the x-ray signal for quantitative analysis. According to the above equations, for any given peak of energy,  $E_p$ , the peak to background ratio (discounting the effects of absorption) will vary according to the following equation:

$$\frac{I_p}{I_b} \propto \frac{(E_o - E_c)^{1.7}}{(E_o - E_p)}$$

eq. 5-3

The relative increase in  $I_p/I_b$  for three typical elements is shown in Figure 5-1. Increasing  $E_o$ , all other factors remaining constant, will improve the quality of the signal and sensitivity of the analysis for all elements. In practice, the increase of  $E_o$  must be limited because of factors such as damage to the sample and the larger interaction volume produced by higher acceleration voltages. As the beam voltage increases, the size of the interaction volume for x-ray generation increases (see Chapter 2) and this can result in a serious deterioration of the spatial resolution of the analysis and a significant increase in the magnitude of the absorption correction factor. Lower voltages produce lower precision and accuracy because operation close to the critical excitation energy is a situation where intensities are greatly reduced and calculations of ionization efficiency are problematic. The "rule of thumb" usually applied is that  $E_o / E_c \equiv U_o$  (known as the **overvoltage**) should be two or greater for all of the elements present in the sample. For most silicate analyses,  $E_o$  can be set at 15 keV. If Au were to be analyzed quantitatively in a specimen, an increase of  $E_o$  to 20 keV or greater might be desirable.

## 5.2 Measuring the X-rays

The x-rays generated in the specimen emerge from a volume of a few cubic microns (see Chapter 2). In the context of detecting and measuring x-ray intensity, the x-rays can therefore be considered to originate from a point source. All wavelengths (characteristic energies of all elements excited) are generated simultaneously and in all directions. The most basic requirement of an x-ray spectrometer is first to separate the characteristic x-rays from each other, and second to measure their intensity. The separation of each characteristic x-ray from all of the rest is accomplished either by wavelength discrimination (WDS) or by energy discrimination (EDS). The WDS approach, although more time consuming and less flexible, is the most sensitive (precise) and accurate method for quantitative microanalysis.

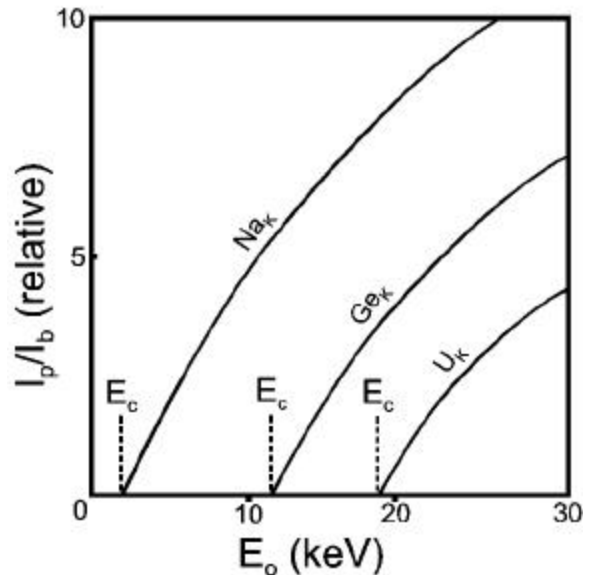


Figure 5-1 Relative peak:background intensities for Na, Ge and U K $\alpha$  x-rays, as a function of acceleration voltage.

### 5.2.1 Diffracting Crystal Spectrometers

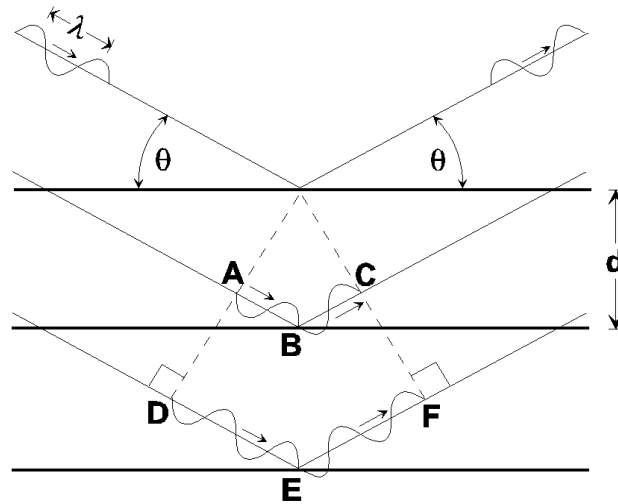
As you all know, a crystalline solid with an interplanar spacing  $d$  will "diffract" x-rays of wavelength  $\lambda$  when the angle of incidence between the crystallographic planes and the x-rays (angle  $\theta$ ) obeys the Bragg equation:

$$n\lambda = 2d \sin \theta \quad \text{where } (n = 1, 2, 3\dots)$$

eq. 5-1

We are most familiar with the Bragg equation vis-à-vis x-ray diffraction studies in which a fixed wavelength ( $\lambda$ ) of radiation is used to determine the "d-spacing" of materials. As shown in Figure 5-2, constructive interference occurs when the length  $ABC = 2d \sin \theta = \lambda$ ;  $DEF = 4d \sin \theta = 2\lambda$ ; etc, etc.

In EPMA, we utilize the Bragg equation both to discriminate x-rays and to focus the discriminated x-rays to an x-ray detector. In essence, we use the Bragg equation in reverse relative to XRD studies. WDS x-ray spectrometers are equipped with one or more "diffracting crystals" of known d-spacing. By moving these crystals relative to the point source of x-rays, the value of  $\theta$  is changed and different x-ray wavelengths are thus diffracted to a detector.



$$n\lambda = 2d \sin \theta$$

(e.g.,  $\lambda = AB = BC$   $2\lambda = DE = EF$ )

Figure 5-2 Schematic diagram illustrating Bragg's Law for x-ray diffraction.

Note that the Bragg equation needs to be modified slightly to account for refraction effects for higher order diffractions (with different energies) depending on the material of the diffracting crystal.

Theoretically,  $\theta$  can be varied from  $0^\circ$  to  $90^\circ$ , but in practice there are mechanical and other practical limits (e.g., the need for constant take-off angle and general space problems around the electron column) to the incidence angle that the diffracting crystals can present to the x-rays. For example, in our CAMECA microprobe the range is approximately  $13^\circ$  to  $56.5^\circ$  for  $\theta$  ( $\sin \theta = .2199$  to  $.8838$ ). If we select 15 keV as the acceleration voltage, the x-ray wavelengths generated within the sample can range from 1 to 15 keV, corresponding to a range in  $\theta$  from  $12.397^\circ$  to  $0.827^\circ$  ( $\theta = 12397/E_0$ ).

Given the limit in the range of  $\lambda$ , we access the wide range of wavelengths by utilizing different diffracting crystals, each with a different  $d$ -spacing. The crystals currently installed on our microprobe are listed in the table below.

Abbreviation	Name	Composition	(hkl)	2d(A)
LiF	lithium fluoride	LiF	(200)	4.0267
PET	pentaerythritol	C(CH <sub>2</sub> OH) <sub>4</sub>	(002)	8.742
TAP	thallium acid phthalate	TIHC <sub>8</sub> H <sub>4</sub> O <sub>4</sub>	(1010)	25.745
ODPb	lead stearate	(film) -	100.70	
PC1	PC1	Si-W	-	60.4
PC3	PC3	Mo-B <sub>4</sub> C	-	200.5

Z	El	??Ka??Å	LiF	PET	TAP	ODPb	PC1	PC3	??La??Å
4	Be	114.000						K.57665	
5	B	67.600				K.68326		K.34270	
6	C	44.700				K.45180	K.75179	K.22640	
7	N	31.600				K.31939	K.53124		
8	O	23.620				K.23874	K.39666		
9	F	18.320			K.71315		K.30760		
10	He	14.610			K.56873				
11	Na	11.910			K.46363				
12	Mg	9.890			K.38499				
13	Al	8.339			K.32463				
14	Si	7.125		K.81445	K.27737				
15	P	6.157		K.70376	K.23968				
16	S	5.372		K.61405					
17	Cl	4.728		K.54040					
18	Ar	4.192		K.47913					
19	K	3.741		K.42765					
20	Ca	3.358		K.38387		L.36720			36.330
21	Sc	3.031	K.75274	K.34644		L.31687			31.350
22	Ti	2.749	K.68261	K.31416		L.27714			27.420
23	V	2.504	K.62178	K.28616		L.24510			24.250
24	Cr	2.290	K.56866	K.26172					21.640
25	Mn	2.102	K.52200	K.24024	L.75714				19.450
26	Fe	1.936	K.48083		L.68473				17.590
27	Co	1.789	K.44430		L.62175				15.972
28	Ni	1.658	K.41175		L.56682				14.561
29	Cu	1.541	K.38261		L.51914				13.336
30	Zn	1.435	K.35643		L.47702				12.254
31	Ga	1.340	K.33282		L.43957				11.292
32	Ga	1.254	K.31145		L.40625				10.436
33	As	1.176	K.29204		L.37646				9.671
34	Se	1.105	K.27438		L.34996				8.990
35	Br	1.040	K.25823		L.32600				8.375
36	Kr	0.980	K.24341		L.30430				7.576
37	Rb	0.926	K.22987		L.28488				7.318
38	Sr			L.78443	L.26715				6.863
39	Y			L.73711	L.25103				6.449
40	Zr			L.69387	L.23631				6.071
41	Nb			L.65430					5.724
42	Mo			L.61798					5.407
43	Tc			L.58463					5.115
44	Ru			L.55388					4.846
45	Rh			L.52550					4.597
46	Pd			L.49923					4.368
47	Ag			L.47486					4.154
48	Cd			L.45222					3.956
49	In			L.43114					3.772
50	Sn			L.41148					3.600

Table 5.2. Sine theta and wavelengths (Angstroms) values for x-ray lines analyzed on various crystals available for the CAMECA microprobe.

Table 5.2, on the facing page, lists the ranges of elements accessed by each of these crystals on our CAMECA microprobe. The values listed are in terms of  $\sin^2\theta$ . Notice that if we restrict our attention to the  $K\alpha$  x-rays, then ODPb, as well as the multi-layer crystals PC1 and PC3, are used for elements lighter than oxygen. We typically use TAP for analysis of fluorine to silicon; PET for silicon to scandium; and LiF for scandium to rubidium.

The x-rays generated in the specimen emerge at all values of take-off angle (the angle between the specimen surface and the x-ray, usually denoted by the symbol  $\psi$ ) between  $0^\circ$  and  $90^\circ$ , and do not constitute a parallel beam. Consequently, a single diffracting crystal of finite dimensions set in a fixed orientation in the path of these divergent x-rays would reflect a range of wavelengths as shown in Figure 5-3. A detector placed as shown would detect only those x-rays of wavelength  $\lambda_2$ . As the crystal is rotated, the diffracted x-rays would span a range of wavelengths. While such an arrangement theoretically provides the rudiments of a "wavelength dispersive system", it fails in practice since only the x-rays diffracted from a small fraction of the crystal surface ever reach the detector. The resulting signal would be far too weak for precise analysis. An alternative would be to increase the size of the detector window (so as to allow collection of more x-rays), but that option would compromise the wavelength discrimination. A modified design that somehow focuses more x-rays of a fixed wavelength to the detector is needed.

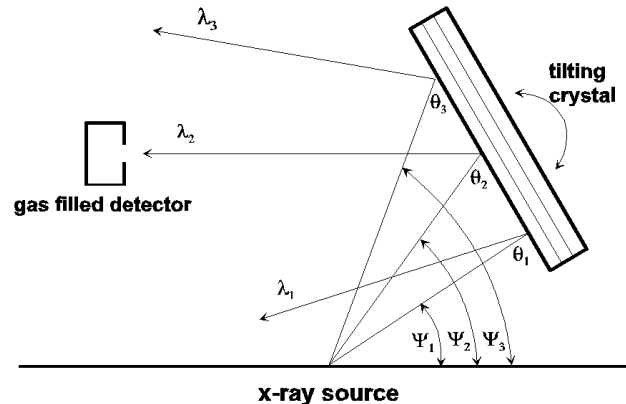


Figure 5-3 Schematic diagram of a crude (flat crystal) WDS spectrometer.

The satisfactory solution to the focusing problem is what is known as a *Johannson fully focusing spectrometer*. The concept behind this type of spectrometer is to maximize the number of x-rays (of a fixed wavelength) that can be focused to a detector. A fully focusing spectrometer consists of the following arrangement.

The source point (S), and the surface of the diffracting crystal, and the x-ray detector window are all constrained to lie on the circumference of a common circle known as the focusing, or *Rowland Circle* (radius =  $R$ ). The diffracting crystal is bent so that the reflecting atomic planes have a radius of curvature equal to  $2R$ . The surface of the diffracting crystal is ground to a radius of curvature  $R$  so that all points on the surface lie on the Rowland circle.

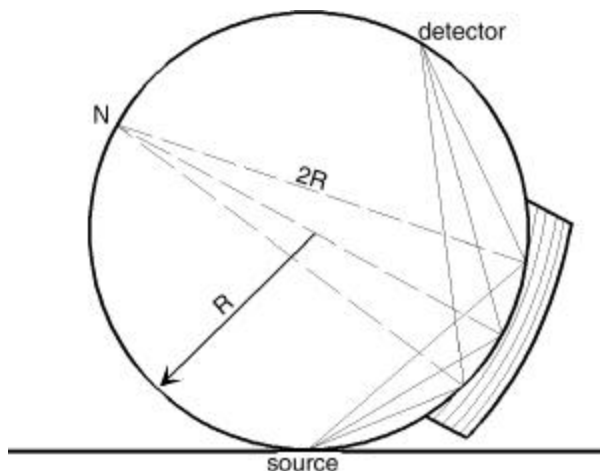


Figure 5-4 Schematic arrangement of a "fully focusing" x-ray spectrometer.

In the above diagram, point N is the center of curvature for all of the diffracting planes in the crystal, so that all normals to these planes pass through N. Since "equal angles subtend equal arcs" the cone of x-rays which diffract at angle  $\theta$  from each of the planes along the Rowland circle are brought back together (i.e., focused) at the point on the Rowland circle occupied by the detector. This arrangement clearly maximizes the number of x-rays of selected wavelength that are diffracted to the detector, thereby significantly increasing the strength of the x-ray signal generated by the sample.

Although the principle of a Johannson spectrometer is straightforward, in practice it turns out to be impractical owing to the combined requirements of crystal materials with suitable d-spacings that are flexible enough to be bent (to  $2R$ ) and yet hard enough to be ground (to  $R$ ). It turns out that the process of grinding flexible crystals to a radius equal to the Rowland circle on most microprobes (4 to 5 inches) creates submicroscopic stacking faults that severely degrade the focusing power of the crystal. For this reason, a compromise has been made that eliminates the grinding of the crystals to  $R$ . This compromise results in what is called a "*Johann*" spectrometer. Although focusing conditions are not perfectly attained in a Johann spectrometer, if the crystal is made sufficiently small, relative to the Rowland circle, very good wavelength resolution can be achieved. The CAMECA crystals are approximately 1.5" in length.

In addition to the requirements for x-ray focusing and good wavelength resolution, a good spectrometer system must also be one in which the x-rays that are diffracted to the detector are only those coming off the specimen at a fixed take-off angle. This requirement stems from the need to apply corrections for absorption and fluorescence — corrections that requires a constant path length through the specimen. When the constant take-off angle is imposed, the mechanical operation of the spectrometer becomes more complex.

The geometrical movement of the crystal, Rowland circle and detector in the CAMECA microprobe are illustrated in Figure 5-5. The crystal travels along a straight line away from the specimen (P) by movement on a lead screw. As the crystal assembly moves from point P to point C, the crystal is rotated to satisfy Bragg's law. The diameter of the Rowland circle remains fixed, but the center of the Rowland circle migrates along the path marked R. The detector follows the cloverleaf path marked D. The orientation of the detector must also be rotated so that it always looks toward the crystal. The limitations of the spectrometer are determined by the fact that for a Bragg angle of  $0^\circ$  the detector would have to be a point P (i.e., the specimen) and for a Bragg angle of  $90^\circ$ , both the crystal and the detector would have to be at point P.

If the rotation of the crystal is mechanically linked to travel of the entire crystal assembly up and down the lead screw (path P-C in Fig. 5-5), the diffraction angle ( $\theta$  or  $\sin\theta$ ) is determined by the crystal's position along the lead screw. Figure 5-6 illustrates the orientation of the Rowland circle, crystal and detector for the detection of two different x-ray wavelengths. For a given set of instrument parameters (e.g., diameter of Rowland circle, d-spacing of the crystal and take-off angle), the wavelength of x-rays diffracted to the detector is directly proportional to L (the position of the crystal along the lead screw).

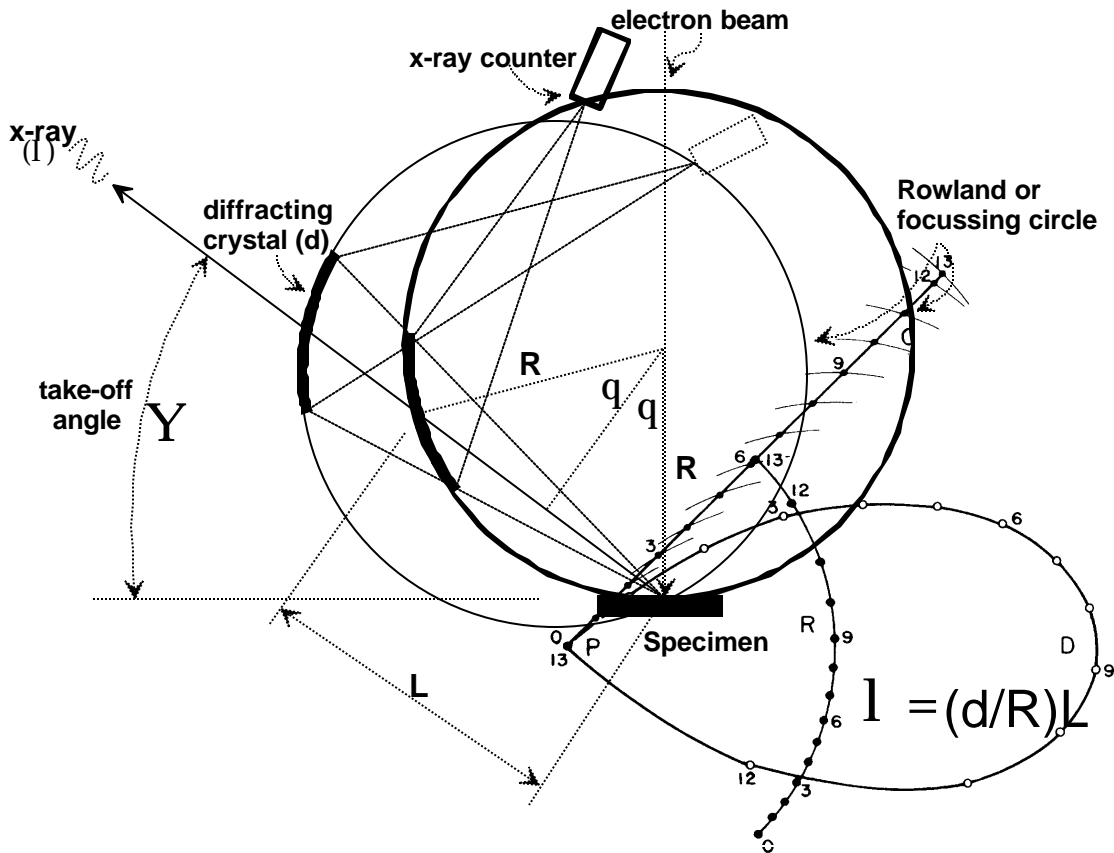


Figure 5-6 Schematic orientation of a Johann x-ray spectrometer at two different wavelength positions.

Figure 5-5 Diagram illustrating the movement of the crystal and the detector relative to the center of the Rowland circle in a Johann x-ray spectrometer.

Most computer-automated microprobes synchronize and keep track of the  $\theta$  position by counting the number of rotations of the lead screw or by counting the number of "motor steps" driving the lead screw. In our opinion, the greatest advantage of the CAMECA instrument is that the position of the crystal, and hence  $\theta$ , is directly read with an optical encoding device. As the crystal assembly moves up and down the lead screw, it travels over a glass plate with etched vernier markings spaced approximately 0.01mm apart. Riding on the crystal carriage is a photocell detector designed to read these ticks and interpolate between them with a precision of  $1\mu\text{m}$ . With this ingenious system, the computer knows precisely where the crystal is and can move it to any desired position with a precision of approximately  $1\mu\text{m}$ . In addition to being precise, the CAMECA spectrometers are also exceedingly fast. A scan through the entire range of  $\theta$  can be done in about 15 seconds.

Additional flexibility is incorporated into modern instruments by allowing the crystal carriage to contain more than one crystal. Although only one crystal can be used at a time, this capability allows the analyst considerable flexibility in configuring the spectrometers for the range of elements to be analyzed. The crystals present on our instrument are given in the following table.

Spectrometers	#1 <sup>1</sup>	#2	#3	#4
	ODPb	TAP	PET	PET
	TAP	PET	LiF	LiF
	PC1			
	PC3			

The analyst must recognize the consequences of all terms in the Bragg equation. For a particular value of  $\theta$ , as the term  $n$  varies from  $n = 1, 2, 3, \dots$ , the order of the reflection varies and so does the value for  $\lambda$ . If the first order ( $n=1$ ) reflection is obtained on a given crystal, there may be several other values of  $\theta$  at which peaks corresponding to this same  $\lambda$  will be found. An important consequence is that for a given setting of  $\theta$  on a particular crystal with fixed  $d$ -spacing, x-rays of different energies which satisfy the same value of the product  $n\theta$  will be diffracted.

An example: Consider sulfur in an iron - cobalt alloy. The S K $\alpha$  ( $n=1$ ) peak occurs at  $5.372\text{\AA}$  and the Co K $\alpha$  ( $n=1$ ) peak occurs at  $1.789\text{\AA}$ . The third-order Co K $\alpha$  ( $n=3$ ) line falls at  $3 \cdot 1.789\text{\AA} = 5.367\text{\AA}$ . The S and third-order Co peaks are so close in wavelength that they cannot be separated by a WDS spectrometer and hence both will be diffracted to the x-ray detector. Although the wavelengths are very similar, these two x-rays differ in energy by a factor of more than three. Fortunately, the x-ray detection system allows these two x-rays to be separated (see Pulse Height Analysis).

<sup>1</sup> Spectrometer 1 and 2 are our only spectrometers configured with a 4 crystal holder.

### 5.2.2 Detection of x-rays by gas proportional counters

Once x-rays are diffracted and focused to a detector it is necessary to transform the x-ray photons into a measurable electronic pulse and then "count" the number of pulses as a measure of the intensity of the x-rays collected by the spectrometer. The type of detector currently used on WDS spectrometers is known as a *Gas Proportional Counter*.

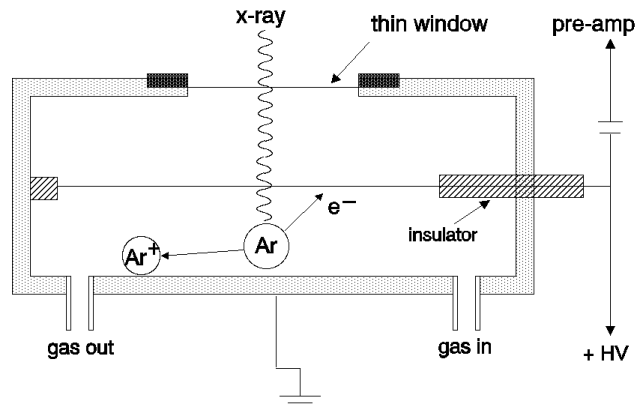
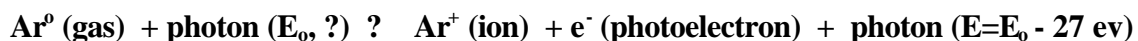


Figure 5-7 Schematic diagram of a gas flow proportional counter or detector.

Reduced to its simplest terms, the gas proportional counter (or detector) consists of a container of gas into which x-ray photons enter through a thin window and cause the gas to ionize. During ionization of the gas, electrons are produced, collected and electronically processed into a measurable "pulse" which serves as a signature of the photon. The diagram to the right illustrates the general features of such a detector. In this type of detector, the ionizable gas actually flows through the container, hence it is known as a *flow proportional detector*. The active gas used in an x-ray detector is most commonly argon.

Special considerations need to be given to the material used for detector windows. The window must consist of a suitable material and be thin enough to be virtually transparent to the x-rays passing through it. At the same time, it must be strong enough to support the pressure gradient between the flowing gas and the vacuum inside the spectrometer itself. In our microprobe, the windows on our light-element spectrometers (Spectrometers #1 and #2) consist of an ultra-thin sheet of mylar or polycarbonate. This ultra-thin window is required in order to allow the transmission of low-energy x-rays, especially those collected by the ODPb and PC crystals (e.g., C, O and even lighter elements). Spectrometers #3 and #4, since they are devoted to more energetic x-rays can utilize a stronger and relatively "less transparent" window consisting of a thin sheet (ca., 10 microns) of beryllium.

Ionization of the counter gas by x-ray photons is the key process in these detectors. As x-ray photons enter the detector they interact with the gas molecules and ionize them (ionization of outermost electrons) according to the following reaction:



The energy of the remaining photon allows this process is repeated, with a loss of approximately 27ev until the incoming photon has expended all of its energy. The individual interactions between photons and Ar atoms differ in detail, but 27ev is the average energy required to create an  $\text{Ar}^+ + \text{e}^-$  pair. It follows that the average number of photoelectrons thus produced will be equal to  $E_0/27$  (and thus proportional to  $E_0$ ). For example:

Element (Z)	$E_0$ of Ka x-ray (ev)	# of $e^-$ produced/photon
Na (11)	1,041	39
Si (14)	1,740	64
Ca (20)	3,690	137
Fe (26)	6,401	237
Zn (30)	8,628	320
Mo (42)	17,462	647

The  $Ar^+$  produced in this process is large and relatively immobile relative to the  $e^-$ , and we can ignore its behavior for the present discussion (we will explain it in more detail later). The electrons created by argon ionization produce the primary signal we are interested in. The number of electrons produced by an x-ray photon entering the detector is not large enough to generate an electronic signal above the ambient "noise". However, because the number of electrons generated per photon has special importance (i.e., the number is related to the energy of the photon), we must find a way to amplify the signal in a linear fashion.

A thin tungsten wire is located along the central axis of the detector and kept at a high positive potential relative to the wall of the detector. The electric potential thus produced (a.k.a., *the detector high voltage*) attracts the electrons produced by the x-ray ionization process to this collection wire. We use a positive potential of 1400 volts in the detectors on our light-element spectrometers (1 & 2) and a potential of 1900 volts in the detectors on our heavy-element spectrometers (3 & 4). Electrons hitting the collection wire produce a momentary drop in the positive potential of the wire, and this potential drop constitutes the signal of interest.

Owing to the fact that the electrons produced by the ionization process are accelerated toward the collection wire, on their way to the wire they have sufficient energy to cause additional ionization of Ar atoms and formation of additional  $Ar^+/e^-$  pairs. This serves to effectively increase the number of  $e^-$  collected after each photon enters the detector. This implies that the number of electrons reaching the wire is not only dependent on the initial energy of the x-ray photon, but also on the potential of the collection wire.

Figure 5-8 describes the relationship between the voltage applied to the detector and the resultant amplification of the number of electrons generated en route to the collection wire. If no voltage is applied to the detector, the  $\text{Ar}^+/\text{e}^-$  pairs will simply recombine. As the potential between the walls and the collection wire is increased from zero, some electrons are attracted to the wire before recombining. At some potential all of the electrons produced by ionization events are attracted to the wire (rather than recombining). At this point the **gas amplification factor** is unity. An increase in the potential to the wire does

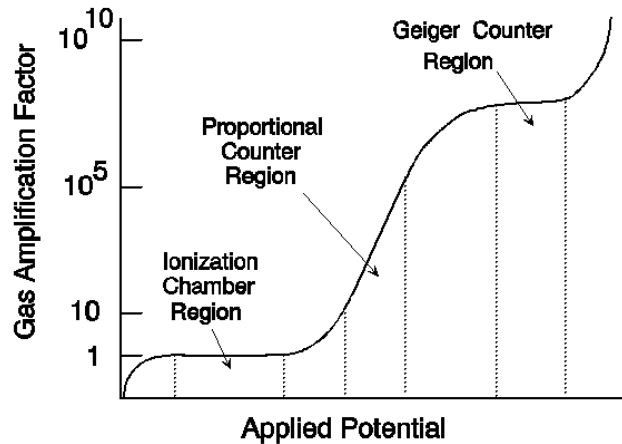


Figure 5-8 Relationship between *gas amplification* and detector voltage (bias) for a gas x-ray detector.

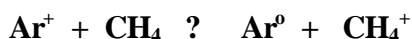
not produce any additional electrons until the acceleration imparted on those electrons is sufficient to produce additional ionization of the Ar atoms. There is thus a plateau in the amplification factor between the voltage required to draw all "original" electrons to the wire and that required to impart sufficient energy to the electrons to produce "secondary" electrons. In detector terminology, this is known as the "*ionization chamber region*". Further increase in the detector voltage results in the attracted electrons having sufficient energy to ionize additional Ar atoms. This produces an **amplification** of the number of electrons available to reach the counter wire. For a certain increase in detector voltage, the rate of increase in the number of electrons reaching the wire (i.e., the gas amplification factor) is constant. In this region, the number of avalanche electrons per primary electron is amplified in a linear fashion and the electrons do not interfere with each other as they travel to the collection wire. In this region the primary signal is increased by a factor of  $10^2$  to  $10^5$  (strong enough to be measured), and most importantly, **the strength of the signal remains proportional to the energy of the incoming photon.**

If detector voltage is increased past the proportional range, then the electrons become involved in multiple avalanches and the avalanched electrons begin to interact (i.e., repel) each other. Electron repulsion serves to destroy the linearity of the amplification factor. In detector terminology, this range of detector voltage is known as the "*Geiger counter region*". In this region, the signal is very strong and this has advantages for other purposes, but not ours, because we need to maintain the characteristic signature of the signal, i.e., we want the size of the pulse (voltage drop on the wire) to remain proportional to the energy of the x-ray which produced the ionization.

### 5.2.3 Counter Gas

The active gas in proportional counters is argon, but it turns out that some other polyatomic "quenching" gas must also be present. In our detectors, we use what is known as '**P-**

10" gas which is a mixture of 90% Ar and 10% CH<sub>4</sub> (methane). The purpose of the quenching gas is twofold: First of all, it prevents the generation of unwanted signals from the Ar<sup>+</sup> ions. The excited Ar<sup>+</sup> ions emit photons in the UV wavelength and since Ar is relatively transparent to UV radiation, most of these photons would reach the walls of the detector if they were not absorbed by methane. If they did reach the walls, they would cause the metal to release photoelectrons, and these electrons would produce an unwanted contribution to the avalanche of electrons reaching the counting wire. The CH<sub>4</sub> molecules absorb UV radiation efficiently and prevent this phenomenon from occurring. Another reason for adding methane is that the CH<sub>4</sub> molecules have a lower ionization energy than Ar. Consequently, the collision of an Ar<sup>+</sup> ion with a CH<sub>4</sub> molecule is likely to result in electron transfer that neutralizes the Ar<sup>+</sup> ion according to the following reaction:



Without this process going on in the counter, the migration of Ar<sup>+</sup> ions to the walls of the detector would give rise to additional photon or electron emission at the cathode. Since the Ar<sup>+</sup> migration to the cathode is slow relative to the generation of the useful signal of electrons at the anode, this effect would be a spurious delayed contribution to the main signal. The CH<sub>4</sub> ions also migrate to the cathode, but they do not cause electron or photon emission when they collide with the wall. Instead, the energy left over after the ion is neutralized causes dissociation to H<sub>2</sub>, CH<sub>2</sub> and C. Since this dissociation is not reversed in the detector, the counter gas "ages" and needs to be replenished. This is the reason for constantly replenishing the gas with a flow system.

## 5.2.4 Other Phenomena

Thus far we have explained what goes on in the detector solely in terms of ionization of Argon by incoming x-rays. This process best explains the proportionality between the energy of an x-ray photon and the number of electrons collected at the central wire. You should realize that other processes can take place in the detector, and some of these can produce interesting results and/or artifacts. Four possibilities need to be considered:

- Some photons might enter the detector undergo a few collisions with Ar atoms and then escape back out of the detector without losing much energy. If this happens, only a few Ar<sup>+</sup>/e<sup>-</sup> pairs are created and essentially no "pulse" is registered. The higher the energy of the photon, the more likely this scenario, but the fraction of times it happens is constant for a given photon energy (i.e., its probability is low and constant for a given x-ray). Furthermore, the probability of losing such an x-ray is the same for counting x-rays on a standard as it is for an unknown. We therefore don't worry about this type of event.
- If the energy of the incoming photon is greater than E<sub>C</sub> for an argon K-shell ionization (3.203 keV), then the photon may excite an Ar-Kα or an Ar-Kβ (less likely) x-ray

photon. Note that only the Ka x-rays from elements with  $Z \geq 19$  have sufficient energy to excite Ar-Ka x-rays. If such an event occurs, **and if** the Ar-Ka x-ray escapes from the detector, an amount of energy is lost from the detector equal to the energy of the escaped Ar-Ka x-ray (i.e., 2.958 keV). The initial x-ray would still create  $\text{Ar}^+/\text{e}^-$  pairs, but the number of such pairs will be less than should have been produced. In this case, a pulse is still collected, but its energy is less than that of the incident photon by an amount equal to the energy of the Ar-Ka photon. The total number of the weaker pulses makes up what is called the *argon escape peak*.

- The same sequence of events as in the scenario above, but in this case the Ar-K $\alpha$  photon does not escape from the detector but is totally consumed by ionization events making  $\text{Ar}^+/\text{e}^-$  pairs. In this case the total number of  $\text{Ar}^+/\text{e}^-$  pairs is the same as it would have been if no Ar-K $\alpha$  ionizations occurred (i.e., no net loss of energy).
- A K-shell ionization of Ar occurs, but the Ar-Ka x-ray is internally consumed by the atom and an Auger electron is produced. The Auger electron will most likely be totally absorbed within the gas detector creating  $\text{Ar}^+/\text{e}^-$  pairs. As long as this happens, there is no net loss of energy and the recorded pulse voltage would be representative of the initial incoming x-ray.

Considering all of these possible scenarios we should conclude that the measured signal from the detector would contain a major "pulse" whose voltage is proportional to the energy of the initial incoming x-ray photons. If the initial photons have an energy greater than the critical excitation energy for Ar-Ka ionization, the detector will produce two pulses -- one proportional to the energy of the incoming x-rays and another displaced to lower voltage corresponding to the argon escape peak.

Lets illustrate the operation of a gas proportional detector with a simple, but relevant example. An electron microprobe operator wishes to analyze a Cr-spinel  $(\text{Fe,Mg})(\text{Cr,Al})_2\text{O}_4$  grain from an ultramafic rock. A potential problem exists because of interference between Al and Cr x-rays as indicated in the table below:

X-ray	?	E (keV)
Al Ka	8.340Å	1.487
Cr Ka	2.290Å	5.414
Cr K $\beta$	2.085Å	5.946
Cr K $\beta$ (n=4)	8.340Å	5.946

Notice that the 4<sup>th</sup> order Cr K $\beta$  x-ray has the identical wavelength as Al Ka. Therefore, when the x-ray spectrometer is "tuned" to the wavelength for Al Ka, it will also be tuned to the wavelength for the 4<sup>th</sup> order Cr K $\beta$  x-ray. The x-ray detector will then "see" both Al and the Cr x-ray photons.

In order to illustrate the output from the detector, let's assume that we can adjust the amplifier gain so that the output pulses (measured in volts) are numerically equivalent to the energies of the incoming photons (measured in keV). In other words, we adjust the amplifier gain to give 1000 eV/V. With such a setup, an Al  $K\alpha$  photon ( $E=1.487\text{keV}$ ) will produce a detector pulse of 1.487 volts.

The detector output on the spectrometer tuned to Al would appear as shown in Figure 5-9. Proceeding from left to right (low to high voltage) we first encounter the very low energy background "noise" from the detector. This background is always present. At 1.487 volts we see the main pulse from the Al  $K\alpha$  x-rays. At 5.946 volts we see the contribution of the 4<sup>th</sup> order Cr  $K\beta$  x-rays. The pulse located near 3 volts corresponds to the Ar-escape peak resulting from the escape of Ar  $K\alpha$  photons generated by K ionization of Ar by the Cr  $K\beta$  x-rays. The exact voltage of this pulse is 2.988 volts ( $5.946 - 2.958$ ) corresponding to the difference in energy of the Cr  $K\beta$  photons and the Ar  $K\alpha$  excitation energy. Notice that there is no Ar-escape peak associated with Al because the energy of the Al  $K\alpha$  photon is less than that required for a K-shell ionization of Ar.

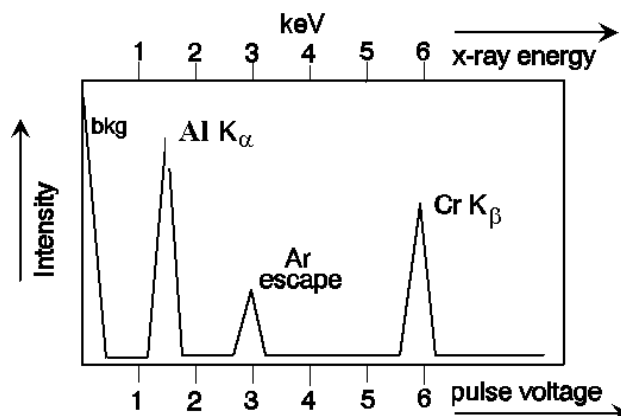


Figure 5-9 Schematic output from a proportional x-ray detector showing pulses for Al  $K\alpha$ , Cr  $K\beta$  and the argon escape peak.

Given the complexity of the detector output, it is reasonable to ask *'how can we ever utilize this signal to quantitatively analyze only aluminum?'* The answer to this dilemma lies in the output itself -- namely the fact that the different pulses have significantly different energies. If we could "filter" the detector output by restricting the range of energies of the pulses that will ultimately be counted, we could effectively eliminate all of the pulses except the one of interest (in the above example, the Al pulse).

Note however, that if the interfering line is of the same diffraction order as the line we wish to analyze, not only will the wavelength be the same, but also the energies will be the same. This situation cannot be remedied by energy filtering and a correction in software must be utilized. See Donovan, et al. 1993.

### 5.3 Pulse Height Analysis

The filtering of the energies of the pulses generated in a proportional detector is accomplished with a **Pulse Height Analyzer (PHA)**, or as it is occasionally referred to a **Single Channel Analyzer (SCA)**. After linear amplification, a detector pulse is fed into the PHA. This electronic device allows the passage of pulses in a selected energy range,  $E \pm \Delta E$ , to the final counting circuits while blocking all pulses outside this preselected range of energy. The

energy  $E$  is called the **threshold** or **baseline** and the interval  $\Delta E$  is called the **window**. The PHA effectively eliminates all pulses with energy below the threshold (baseline) and above the upper limit of the window.

At this point it is necessary to introduce the concept of time into our discussion of electronic processing of x-ray signals. Although the generation of characteristic x-rays by high-energy beam electrons seems almost instantaneous, you need to recognize that only a small fraction of the x-rays generated in the sample ever reach the diffracting crystal and the detector. Those that do reach the detector are separated from one another by finite, albeit short, amounts of time. For the purposes of quantitative analysis, as the concentration of an element in the sample increases, so does the number of x-ray photons characteristic of that element reaching the detector. We are thus interested in the **count rate** (i.e., # of photons per unit of time detected by the spectrometer). Use of the term "count rate" implies a finite interval of time between the arrivals of successive photons into the detector. Indeed, in order for the PHA and counter to function, there must be distinct time intervals between "counting events".

Figure 5-10 illustrates both the shape and time parameters typically associated with the output of the x-ray detector and its amplifiers. The point to recognize here is that these electronic devices take time to form an electronic pulse and then recover from that pulse. We see in part (a) that the initial detector signal consists of a "momentary drop" in the positive potential on the detector wire. After processing by the main amplifier, this initial pulse is transformed into a roughly Gaussian peak in terms of voltage as a function of time. Note that the time frame involved with the pulse leaving the main amplifier is on the order of .3 microseconds ( $3 \times 10^{-7}$  seconds - a short, but finite time period).

A better understanding of Pulse Height Analysis can be gained from Figure 5-11. In this schematic diagram, three different detector "events" produce pulses. The first event to occur (I) produces a pulse of approximately 4 volts, the second (II) about 6V, and the third (III) about 8V.

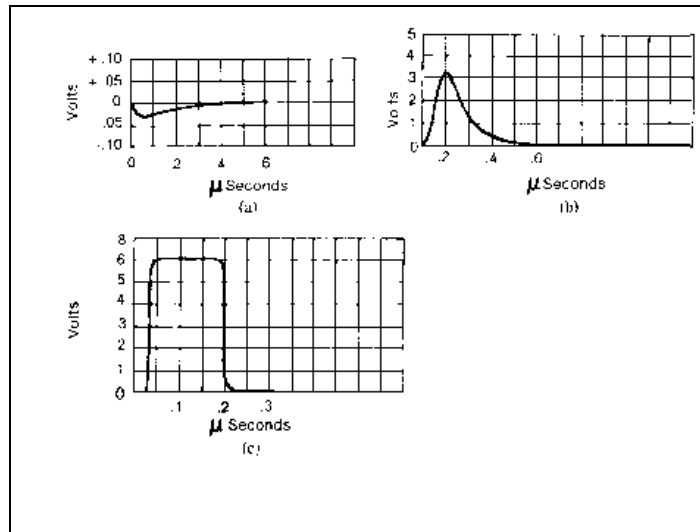


Figure 5-10 Typical WDS x-ray detection pulse shapes. (a)

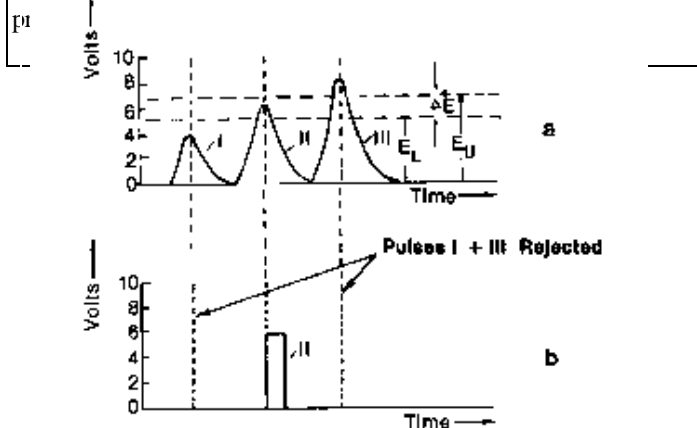


Figure 5-11 Schematic illustration of the operation of a pulse height analyzer (PHA).

Lets say that the "event" we are interested in counting produces the 6V event. In this case we are interested in counting x-rays that have energies resulting in a detector pulse voltage of 6 volts. The lower energy pulse might be due to an argon escape peak while the higher energy pulse might be due to a high-order x-ray from another element present in the sample. In order to filter out all pulses except the peak of interest (i.e., II) we can set the threshold (baseline) of the PHA to 5 volts. This means that the PHA will "reject" all pulses with voltages of less than 5 volts, thereby rejecting all type I events. We can further set the window, as in this case, to 2 volts. This means that all pulses with a voltage greater than 7 volts are rejected (i.e.,  $5 + 2 = 7$ ), thereby rejecting all type III events. With this PHA setting, over the time we wish to count x-rays all detector pulses less than 5V or greater than 7V are rejected -- leaving only the pulses of interest to ultimately reach the counter.

In computer-automated microprobes, the PHA settings (baseline and window) are set by the operator prior to an analysis. Each element in the analysis will have a unique value for the baseline and window, and those values will be different on different spectrometers and detectors. In principle, we want  $\Delta E$  to be narrow enough to exclude all possible interfering events taking place in the detector, but wide enough to always ensure that all of the peak of interest is included. A big advantage of computer-based electronics is that the operator can actually view a pulse spectrum and see the consequences of setting a particular baseline and window for the PHA. In setting up your analyses, you will have to either accept our "default" values or adjust the PHAs for each element in your analysis.

In practice, today's EPMA softwares allow the analyst to simply default to baseline and window values as suggested by the microprobe's automation. The operator need only be careful about selecting parameters such as whether the window be "wide" or "narrow" ("medium" to "wide" would be a general application of PHA discrimination, whereas "narrow" would be chosen for a specific case where a problem is known to exist); whether or not the upper threshold is needed (for example, in the case of x-rays energies greater than 6keV when there is little likelihood of a high-order x-ray problem, many facilities will simple set the baseline to a fixed value to avoid noise); **or** whether the window should remain stationary or move with the spectrometer as it tunes from one wavelength to another. This latter case should be the general rule. That is, for a specific spectrometer with some chosen value for the window, the window does need to move with the anticipated location of the amplified pulse. For example, for magnesium and silicon, both of which can be measured with the same TAP spectrometer, the Mg pulses will be amplified to a value like 1.2V, whereas Si will be amplified to 1.7V ... therefore the window need move from one value to the other. Just how these parameters are taken care of varies from one manufacturer to another ... but the concepts remain the same.

### 5.3.1 Dead Time

The above discussion concerning the formation of discreet electronic pulses corresponding to characteristic x-ray photons as a function of time begs the question, "*what if an x-ray photon arrives in the detector while the detector and associated electronics are busy processing a previous event?*" The answer is simple, but discouraging -- the second photon is

simply not counted and is thus "lost". It is important to understand these lost counts and ultimately make a correction for them.

Consider counting rates of 10,000 counts per second (cps). If the 10,000 photons involved were uniformly distributed in time, they would enter the detector at intervals of  $10^{-4}$  seconds. Reference to Figure 5-10 shows that this is ample time for the system to recover between arrivals of each photon. However x-ray production in the specimen is a random process, and the photons will not enter the detector at uniform intervals. This forces us to consider the possibility that photons might enter the gas counter at very closely spaced intervals of time. When that happens only one pulse may be registered and we have effectively lost some counts. In order to quantify this problem in the most straightforward manner it is useful to consider two approximations.

1. The production of x-ray photons by electron bombardment is a random process (by which we mean that although the average number of photons produced under given conditions measured over a relatively long period of time is reproducible, the production or non-production of a photon during a short period of time is random). For the average count rates we typically operate at (usually  $> 100\text{cps}$ ), one second can be considered to be a long time. Let  $t$  represent a short fraction of a second (e.g., in the microsecond range). Owing to the random character of x-ray production, it follows that the probability of producing one photon during  $t$  is much greater than the probability of producing two photons and very much greater than producing three photons, etc., etc. Consequently, it is a reasonable approximation for us to consider that lost counts are all due to double coincidence and to ignore the much less probable losses due to triple, quadruple, etc., etc. coincidences.
2. We have seen that each time a photon enters the gas counter it causes the production of an electric signal which is internally amplified in the counter itself (the gas amplification factor). The resulting electrons collected by the counter wire are subsequently processed by a series of amplifiers and the PHA. All of this electronic processing requires a finite amount of time to recover from the disturbance caused by one photon before it can respond to a second photon. Each system has, therefore, what we call a characteristic *dead-time* period, and it is because of this dead time that counts are lost. The longer the dead-time and the higher the average count rate, the greater the proportion of counts lost.

The term dead-time is commonly used rather loosely. There are really several "times" characteristic of any counting system that we should be aware of. The definitions that follow and the diagram below should be helpful in explaining what is meant by these times.

***rise-time:*** the time interval after the arrival of a photon for the resulting pulse to reach 90% of its maximum height.

***dead-time:*** the time interval after the arrival of a photon during which no measurable response (however weak) is registered in response to a second photon.

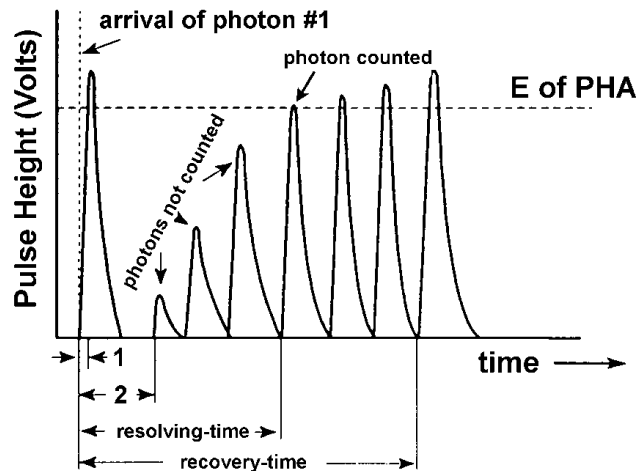


Figure 5-12 Illustration of the various *times* involved with detection of detected pulses. 1 = *rise time*, 2 = *dead time*.

***resolving-time:*** the time interval after the arrival of a photon for the pulses due to the arrival of a second photon to reach a height sufficient to be counted by the PHA. Clearly, if a PHA system is being used it is really the resolving time that is of interest rather than the "dead time" (*sensu stricto*). "Dead time" is often used when resolving time is meant, and we will probably be guilty of interchanging the two as well.

***recovery-time:*** the time interval after the arrival of a photon for the pulses due to the arrival of a second photon to reach its maximum height.

Another way of defining these terms is to say:

*"(only) after the **dead-time** has elapsed can a second pulse occur; (only) after the **resolving-time** has elapsed can a second pulse be counted; (only) after the **recovery-time** has elapsed can a second pulse realize its full amplitude (proportional to the energy of the photon)."*

The first photon (#1) is assumed to enter the detector at  $t_0$  after the counting system is fully recovered from any previous work. The resulting pulse is therefore fully developed. If photon #2 enters the system within one dead-time unit from  $t_0$ , no response at all is possible from the detector. If photon #2 enters the system just after the dead-time interval has elapsed, a separate pulse is generated, but the pulse height is far from fully developed. If the PHA has a baseline (E) that is higher, no count will be registered in the counter. It is only after a time interval labeled "resolving-time" that the second photon can generate a counting pulse. A time interval equal to the recovery-time is necessary before the second photon can generate a pulse that is truly proportional to the energy of the photon. What is loosely called "dead-time" actually corresponds to resolving time and is clearly a function of detector characteristics and the baseline setting of the PHA system. The effect of dead-time is to give spuriously low counts. The loss of counts resulting from dead-time is generally expressed in an equation such as the following:

$$\frac{(n - n_0)}{n_0 t} = \frac{n}{I}$$

eq. 5-1

where  $n$  is the true # of photons striking the detector in one second,  $n_0$  is the observed # of counts in one second, and  $t$  is the dead-time of the detector. Our gas proportional detectors have a dead-time ( $t$ ) of approximately 2 microseconds. According to the above formula, a  $2 \times 10^{-6}$  sec. dead-time can cause serious ( $> 2\%$ ) loss of counts when the count rate exceeds 10,000 counts per second (cps) (see table below).

$n_0$ (cps)	$n_0 / n$ (for $t = 2 \mu\text{sec}$ )
$10^2$	0.9998
$10^3$	0.9980
$10^4$	0.9800
$10^5$	0.8000

During a quantitative analysis, the software will make a correction for the number of counts lost due to deadtime (i.e., it calculates  $n$  based on  $n_0$  and  $t$ ). You should realize, however, that the values typical labs use for dead-time ( $t$ ) are not very accurate. It is therefore important to minimize the problem by avoiding excessive count rates (e.g.,  $>10^4$  cps). It is also important to minimize the dead-time effect by minimizing the count rate difference between the standard and the unknown, especially if the deadtime calibration is not accurately known. Normally deadtime can be accurately calibrated, especially on CAMECA instruments because they have a special "imposed" fixed deadtime that can be used to "mask" variations in the intrinsic deadtime of the detector and pulse processing electronics.

The components discussed in this chapter are summarized in the diagram below.

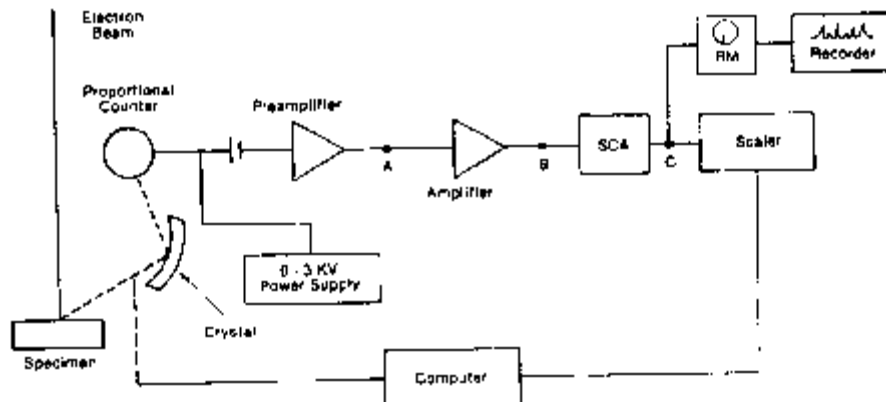


Figure 5-13 Block diagram for a typical wavelength discriminating x-ray spectrometer and counting system.